







# SOME ASPECTS OF VICTORY DAY 2024 GEOMAGNETIC STORM OCCURRED ON MAY 10–12, 2024, USING SATELLITE AND GROUND-BASED DATA

A. A. Chernyshov<sup>\*1</sup> , M. V. Klimenko<sup>2</sup> , A. A. Sinevich<sup>1,3</sup> , A. V. Timchenko<sup>2</sup> , I. A. Nosikov<sup>2</sup> ,  
D. V. Chugunin<sup>1</sup> , and I. S. Yankovsky<sup>2</sup>

<sup>1</sup>Space Research Institute of the Russian Academy of Science, Moscow, Russia

<sup>2</sup>West Department of Pushkov Institute of Terrestrial Magnetism, Ionosphere and Radio Wave Propagation of the Russian Academy of Sciences, Kaliningrad, Russia

<sup>3</sup>Pushkov Institute of Terrestrial Magnetism, Ionosphere and Radiowave Propagation of the Russian Academy of Sciences, Troitsk, Moscow, Russia

\* **Correspondence to:** Alexander Chernyshov, [achernyshov@cosmos.ru](mailto:achernyshov@cosmos.ru)

**Abstract:** The presented work examines the extreme geomagnetic storm that occurred during May 10–12, 2024, following solar flares on May 8–9, 2024, hence named the Victory Day Storm. This event, marked as the most intense geomagnetic storm of the 21st century to date, caused significant disturbances not only in the auroral zone but also in the subauroral and mid-latitude ionosphere. Using data from satellites, ground-based ionosondes, Global Navigation Satellite System (GNSS) receivers, and all-sky cameras located in the Kaliningrad region, this research tracks how the coronal mass ejection from the Sun led to substantial changes in ionospheric plasma density, structure, and dynamics. Notably, auroras were observed in the subauroral and mid-latitudes, which is a rare phenomenon at these latitudes, providing valuable information on the ionospheric response to extreme geomagnetic activity. Swarm and DMSP satellite data identified polarization jet/SAID as U-shaped structures on ionograms, while Strong Thermal Emission Velocity Enhancements (STEVE) was observed by an all-sky camera along with increased Rate of Total Electron Content Index (ROTI). A diffuse aurora with a moving omega structure, as well as ray and corona auroral features, were observed, accompanied by a significant ROTI increase and enhanced scattering of the auroral Es layer on ionograms.

**Keywords:** Extreme geomagnetic storm; Optical phenomenon, Satellite and ground-based means, Solar-Terrestrial Relations, Ionosphere, Auroras, STEVE, PJ/SAID.

**Citation:** Chernyshov A. A., Klimenko M. V., Sinevich A. A., Timchenko A. V., Nosikov I. A., Chugunin D. V., and Yankovsky I. S. (2025), Some Aspects of Victory Day 2024 Geomagnetic Storm Occurred on May 10–12, 2024, Using Satellite and Ground-Based Data, *Russian Journal of Earth Sciences*, 25, ES5011, EDN: TENTPH, <https://doi.org/10.2205/2025es001009>

## Introduction

The 2024 geomagnetic storm has become one of the most notable space weather events in recent history. This storm, occurring from May 10 to May 12, 2024, was triggered by powerful solar flares and coronal mass ejections (CMEs), marking the peak of the 25th solar cycle. It is now recognized as the most intense geomagnetic storm of the 21st century. Understanding the complex processes in Earth's magnetosphere, atmosphere, and ionosphere during such events is essential not only for scientific research but also for mitigating their potential impacts. Following the tradition of naming storms after their most impactful day, we refer to this event as the “Victory Day 2024 Geomagnetic Storm” after the solar flares that erupted on May 8–9, 2024, leading to significant impacts on Earth. Victory Day is a holiday that commemorates the Soviet Union's victory over Nazi Germany on May 8 (May 9, Moscow Time) in 1945. During this storm, auroras were seen in unexpected locations, including places like Armenia, Brazil or Mexico for which such optical processes are extremely rare [Carmo *et al.*, 2024; Chernyshov *et al.*, 2025; Gonzalez-Esparza *et al.*, 2024], as well as an approximately fivefold decrease in the F2-layer electron density over Irkutsk due to huge enhanced recombination rates, which is not typical under normal conditions [Yasyukevich *et al.*, 2025].

## RESEARCH ARTICLE

Received: April 21, 2025

Accepted: July 2, 2025

Published: October 7, 2025



**Copyright:** © 2025. The Authors. This article is an open access article distributed under the terms and conditions of the Creative Commons Attribution (CC BY) license (<https://creativecommons.org/licenses/by/4.0/>).

Historical events like the 1859 “Carrington Event” demonstrate the global reach of geomagnetic storms. During that time, ionospheric disturbances caused widespread telegraph failures, and operators even received electric shocks [Carrington, 1859]. Furthermore, the event created auroras visible as far as the Caribbean and Tahiti, marking the first known connection between large solar flares and terrestrial disruptions.

More recent examples include the 1989 storm, which led to a major power outage in Quebec. A significant CME triggered a geomagnetic storm that knocked out control of some polar-orbiting satellites and tripped circuit breakers on Hydro-Quebec’s power grid, paralyzing transport systems [Bolduc, 2002]. The “Halloween Storm” of October 2003 was the most powerful geomagnetic storm in 21st century until 2024. It caused significant ionospheric disturbances, impacting satellites and navigation systems, though its effects on Earth’s power infrastructure were mitigated by lessons from the Quebec blackout [Horvath and Lovell, 2010].

The *Dst* index dropped to a minimum of  $-412$  nT on May 11, 2024, compared to  $-383$  nT in October 2003, making the Victory Day 2024 Geomagnetic Storm the most intense of the 21st century. Many satellites were placed into safe mode, and Starlink warned of degraded service during the storm due to high solar activity. Navigation systems and radio waves were disrupted, and geomagnetically induced currents (GICs) caused disturbances in power grids and pipelines, impacting sensitive individuals. Geomagnetic storms affect thermosphere, ionosphere, and magnetosphere, with varying impacts across latitudes. These effects are determined by factors such as magnetic deflections, auroral latitude shifts, and changes in the current system. Though related, these factors interact in complex and nonlinear ways [Rich and Denig, 1992].

In this work, we analyze ionospheric and atmospheric data over Kaliningrad region (East Europe), during the Victory Day 2024 Geomagnetic Storm. So, we focus on the subauroral/mid-latitude ionosphere, which play a crucial role in energy transfer from the poles to the equator during strong magnetic disturbances. This region is key for observing the auroral oval’s expansion and substorm evolution. It experiences sharp changes in plasma density, impacting navigation systems like GPS (Global Positioning System) and GLONASS (Global Navigation Satellite System) and radio communications. During storms, phenomena such as Polarization Jets or Sub-Auroral Ion Drift (SAID), Stable Auroral Red arcs (SAR arcs), and STEVE (Strong Thermal Emission Velocity Enhancements) are observed at these latitudes, indicating substorm processes. Furthermore, subauroral regions are near areas of high population density and economic activity. Disturbances here can cause significant disruptions to power grids and communications, as seen during the 1989 Quebec blackout. Space weather models often struggle with the low statistical significance of severe storms due to limited data from such extreme events. This highlights the importance of studying such events, especially as solar activity is expected to peak in 2024–2025. To fully investigate geomagnetic storms, we use both satellite and ground-based data. Satellites such as DMSP, Swarm, and ACE provide information on solar wind, ionosphere-magnetosphere coupling, while ground-based tools, including ionosondes, GPS/GLONASS receivers, and all-sky cameras, offer temporal variability of high-resolution data on local ionospheric and magnetic field changes. Combining these observations helps to clarify the time evolution and effects of geomagnetic storms. In the presented study, we use data from the Ladushkin scientific observatory of WD IZMIRAN in Kaliningrad region, along with satellite data, to analyze in detail the Victory Day 2024 Geomagnetic Storm’s impact on the ionosphere/upper atmosphere. This paper is the second in a series examining the upper atmospheric and ionosphere response to the Victory Day storm 2024 over Kaliningrad (see [Chernyshov et al., 2025]). In the current study, we provide a more detailed analysis of ionospheric irregularities during the three main storm intervals when STEVE, omega structures, rays, and corona auroral structures were observed over the WD IZMIRAN observatory. Also here for the first time, we use the DMSP satellite data and explicitly prove that there was a polarization jet/SAID and STEVE during this extreme magnetic storm and the observation of STEVE optical emissions, as recorded by the all-sky camera over the Kaliningrad region.

### Characteristics of the Extreme Geomagnetic Event

Data from the ACE satellite, providing details on solar wind and interplanetary magnetic field (IMF) parameters [Stone *et al.*, 1998], is crucial for geomagnetic storm analysis. The study uses this data to evaluate solar wind changes during May 10–12, 2024, storm (see Figure 1a, b, c). Before the disturbance, solar wind speed averaged 350 km/s but increased to ~700 km/s on May 10 and reached ~1000 km/s on May 11, signaling a CME as can be seen from Figure 1b. This speed rise coincided with sudden increases in plasma density and temperature as shown in Figure 1c, forming a shock wave front that caused the storm, reflected in high geomagnetic index values. In Figure 1a, IMF data show that  $B_z$  turned southward at 16:40 UT on May 10, 2024, remaining negative until May 11 with peaks up to ~45 nT, while  $B_t$  reached nearly 73 nT. Negative  $B_z$  enables magnetic reconnection at the magnetopause, causing the polar cap to expand and the auroral oval to move equatorward, recorded by ground-based instruments. The  $B_y$  component of interplanetary magnetic field also shows strong fluctuations when  $B_z$  has a negative value. The solar wind's high speed and dynamic pressure determine the compression of the magnetosphere and the location of the magnetopause. The shock wave associated with solar wind disturbances further intensifies this compression. The negative IMF  $B_z$  component facilitates energy transfer from the solar wind to the magnetosphere, enhancing reconnection processes and driving geomagnetic activity as observed in this study through ground and satellite instruments.

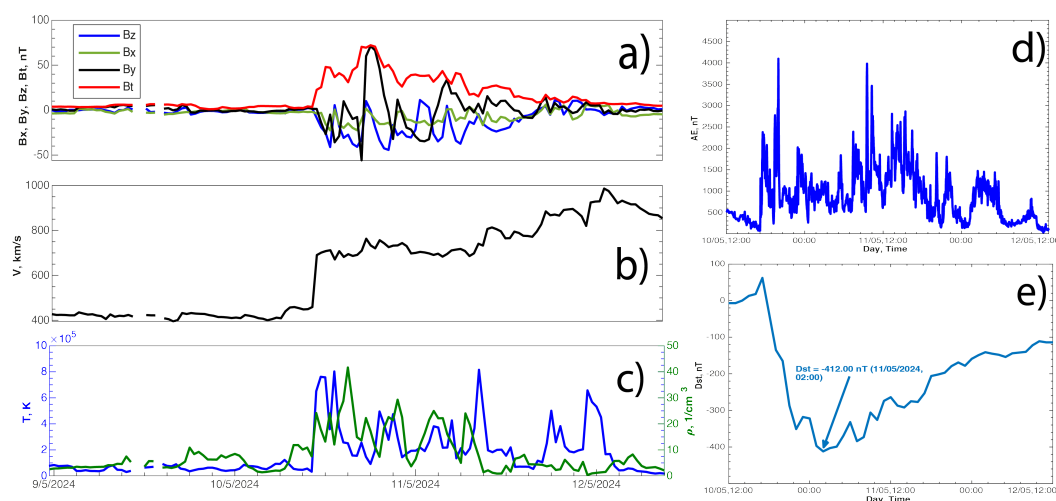


**Figure 1.** Evolution of the geomagnetic index AE (a) and Dst (b) during Victory Day 2024 Storm. Solar wind data: Interplanetary magnetic field (c) where  $B_t$  (red line),  $B_z$  component (blue line),  $B_y$  component (black line) and  $B_x$  component (green line); Solar wind speed (d); Plasma density and Temperature (e) where temperature is the blue line,  $y$ -axis is on the left, and plasma density is the green line,  $y$ -axis is on the right.

During the Victory Day 2024 Geomagnetic Storm, significant changes were recorded in the geomagnetic indices AE and Dst (see Figure 1d, e). The geomagnetic disturbances began on May 10 around 16:00 UT, marked by a sharp increase in the AE index. The AE index, which reflects magnetic fluctuations in the auroral zone due to intensified ionospheric currents along the auroral oval's boundary, rose sharply, reaching over 4,000 nT by evening, signaling a strong storm as is clear from Figure 1d. AE values remained high through the morning of May 11, 2024, peaking again near 4,000 nT before decreasing on the evening of May 11 to values between 300 and 2,000 nT, and ultimately settling below 1,000 nT by May 12. High AE values were accompanied by an expansion of the auroral oval to lower latitudes, making auroras visible in regions where they are rarely seen [Chernyshov *et al.*, 2025; Gonzalez-Esparza *et al.*, 2024].

In Figure 1e, the Dst index, which reflects as a rule ring current intensity, showed the growth phase (Storm Sudden Commencement) began on May 10 at ~16:00 UT and lasted about 3 hour, during which the index increased to 62 nT. After that, at around 19:00 UT,

there was breakup (the initial stage of the active phase called breakup is accompanied by a sharp brightening of auroras) and *Dst* reached a minimum of  $-412$  nT by early May 11 (around 02:00 UT), indicating a very strong geomagnetic storm. The recovery phase with *Dst* index gradually increased but remained below  $-300$  nT until noon on May 11, 2024, finally rising above  $-100$  nT by the end of May 12. Starting on May 8, 2024, heightened solar activity, including X-class solar flares, CMEs, and high-speed plasma streams, was observed. The impact of this activity reached Earth's magnetosphere a few days later, correlating with high *AE* and low *Dst* values and causing auroras, polarization jet/SAIDs, STEVE, GNSS (Global Navigation Satellite System) scintillations, radio disruptions, and more.

### Ground-Based Data

The WD IZMIRAN magnetic-ionospheric observatory, located in the Kaliningrad region ( $54.36^{\circ}\text{N}$ ,  $20.12^{\circ}\text{E}$ ), has a modern array of research instruments. In this work, the analysis of the geomagnetic storm is conducted using data from the Parus-A vertical ionosonde, an all-sky camera, and a dual-frequency GNSS receiver. The all-sky camera captures images approximately every 30 seconds with an automatically adjustable exposure time. This camera is part of the Starvisor network, a project for automated night sky observations through an extensive network of cameras. The Starvisor project website (<http://starvisor.ru/>) provides real-time information about the visibility of auroras, noctilucent and nacreous clouds, meteor showers, and other phenomena at various latitudes across Russia. The Parus-A vertical ionosonde conducts scans every 15 minutes in standard mode. For a more comprehensive analysis, this study also includes ionograms obtained from the DPS-4 digisonde located in Juliusruh, North Germany ( $54.6^{\circ}\text{N}$ ,  $13.4^{\circ}\text{E}$ ). The Juliusruh digisonde is situated at the same latitude as the WD IZMIRAN observatory but approximately  $7^{\circ}$  ( $\sim 650$  km) further west. Therefore, these two locations can observe similar reflection patterns in structure, altitude, and frequency, sometimes with a slight time delay. Note that the instruments and software of the digisonde can determine the direction of incoming signals. The Juliusruh digisonde also operates in a standard 5-minute mode. The dual-frequency GNSS receiver monitors the Total Electron Content (TEC) and its rate of change (ROT) [Pi et al., 1997] over the Kaliningrad region.

Figure 2a shows the initial manifestations of the geomagnetic storm, recorded by both the all-sky camera and the Parus-A ionosonde at 20:00 UT on May 10, 2024. A bright glow with a pronounced maximum against the background of sunset illumination is observed in the camera image. At the same time, data from Parus-A indicate an additional trace in the F-region, featuring a U-shaped structure about 150–200 km above the regular vertical reflection trace at this time. A similar additional trace from the northern direction was observed on the ionogram from the DPS-4 digisonde in Juliusruh as inferred from Figure 3a. These characteristic signs on the camera images and ionograms are indicative of a polarization jet (PJ) [Stepanov et al., 2019] and STEVE [Parnikov et al., 2022]. According to the camera and ionosonde data, PJ/SAID and STEVE signatures were observed over the Kaliningrad region from 20:00 to 20:03 UT, northwest of the observation site, with STEVE moving westward. During this period, GNSS receiver data also indicated an increase in the ROTI (Rate Of TEC Index), peaking to the north of the WD IZMIRAN observatory (see Figure 4a). This indicates that the wall of the PJ/SAID trough was located north of Juliusruh and Kaliningrad. In addition, ionograms showed stratification in the E-region. Reflections from both an auroral-type sporadic *Es* layer and a lower, additional reflection trace were recorded. The additional trace on the ionogram appeared at a virtual height of 106.5 km, with signal frequencies ranging from 1.75 to 3.93 MHz. As can be seen from Figure 3a, the DPS-4 data showed a similar reflection trace originating from the North-North-East (NNE) direction, within the same frequency range.

Figure 2b shows all-sky camera images depicting an omega structure and ionograms recorded at 20:45 UT on May 10, 2024. The omega structure was observed over the Kaliningrad region from 20:43 to 20:47 UT, to the north of the WD IZMIRAN observatory.

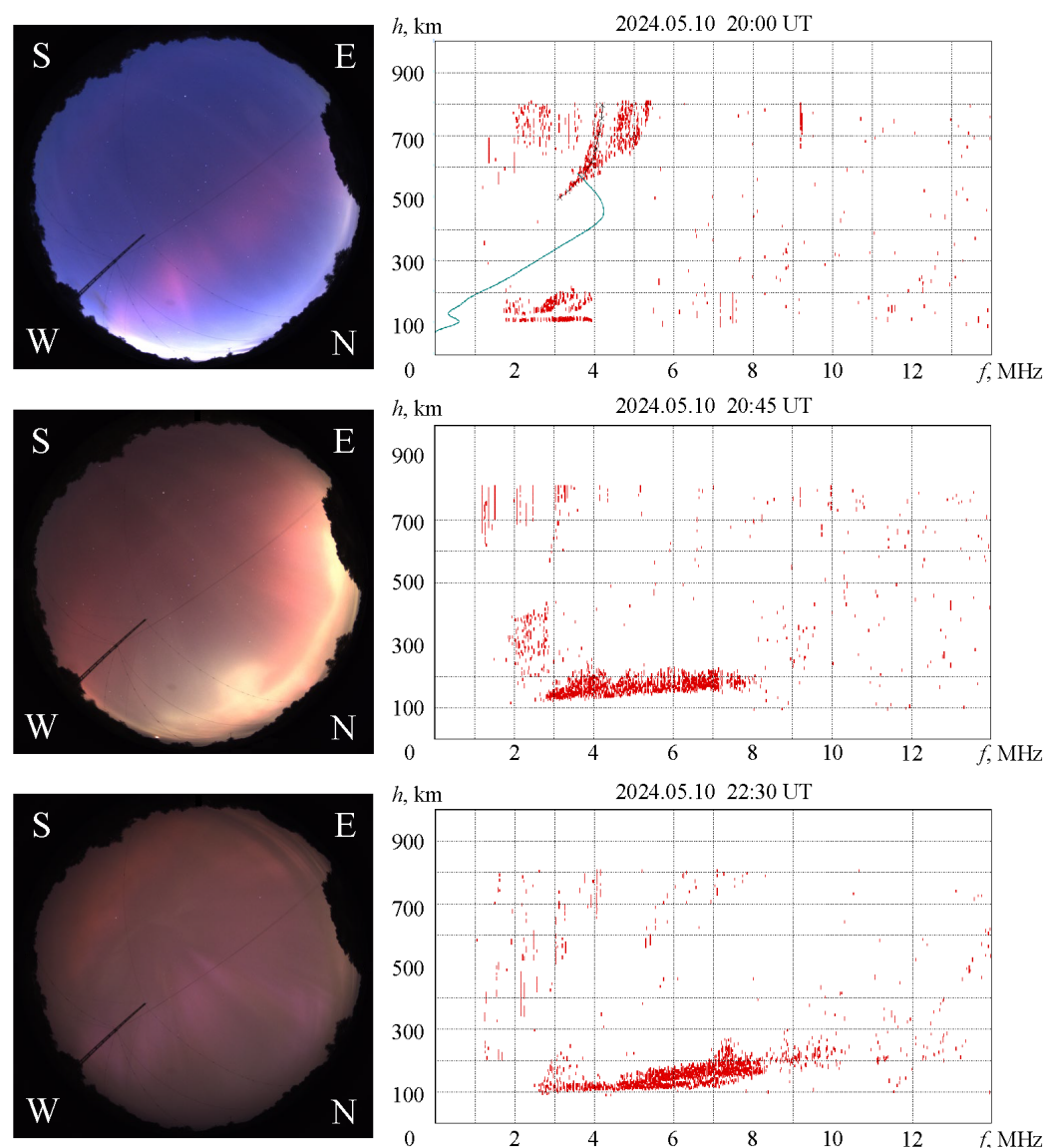


**Figure 2.** All-sky camera images (left panel) and ionograms (right panel) taken from WD IZMIRAN observatory (Kaliningrad region, Russia) at 20:00, 20:45 and 22:30 UT on May 10, 2024. The solid turquoise line corresponds to the reconstructed plasma frequency profile according to manual processing of the ionogram for 20:30 UT.

According to the GNSS receiver data, during the registration of the omega structure, the ROTI exhibited a sharp, short-lived peak exceeding 4 TECU/min as is clear from Figure 4b. The ROTI maximum was located to the northwest of the WD IZMIRAN observatory, consistent with the all-sky camera observations. The all-sky camera data indicate that the omega structure, located at the southern boundary of the diffuse aurora, moved westward. This structure can be classified as an O/T type, that is, a combination of the classic O-type, where poleward lines bend into the shape of the Greek letter  $\Omega$ , and the T-type, characterized by torch- or tongue-shaped lines bending northward [Sato *et al.*, 2017]. However, since the omega structure appears near the edge of the image, accurately determining its type is challenging due to structural distortion and blurriness.

At this time, vertical sounding ionograms from the Parus-A and DPS-4 ionosondes show that the auroral *Es* layer screens the upper layers, causing its trace to scatter in range (latitude and altitude). Unlike other moments on the ionograms (see Figure 2b and 3b), a multi-layered reflection structure from the auroral *Es* is present. In the lower frequency



range (2–4 MHz), reflections predominantly come from the south. In the 4–5.5 MHz range, vertical reflections are mainly observed, while in the upper frequency range (5.5–7 MHz), reflections predominantly come from the north.

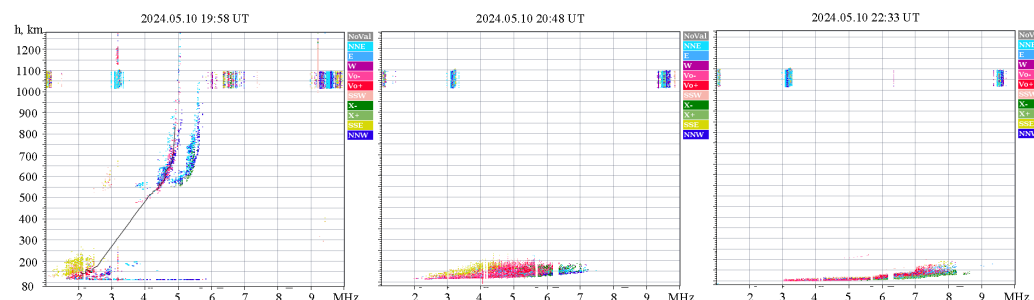


**Figure 3.** Ionograms observed by the Juliusruh digisonde DPS-4 at 19:58 (a), 20:48 (b) and 22:33 UT (c) for 10.05.2024. The solid black line indicates the processed ordinary mode track of the vertically reflected radio signal for 19:58 UT.

Figure 2c shows an all-sky camera image of a ray and corona structures of aurora and an ionogram recorded at 22:30 UT on May 10, 2024. The ray structure was observed over the Kaliningrad region from 22:26 to 23:02 UT, almost at the zenith of the WD IZMIRAN all-sky camera. The detection of this ray structure, characteristic of the inner auroral oval, directly over the WD IZMIRAN observatory indicates a significant equatorward shift of the oval boundary below 50°N latitude. At the same time, the GNSS receivers data recorded the highest and most prolonged increase in the ROTI as seen in Figure 4c. The ROTI value exceeded 4 TECU/min, and the Observatory was at the center of the maximum ROTI growth region. Besides, during the observation of the ray structure, the all-sky camera recorded several short-lived omega structures, although these did not coincide with vertical sounding data. During this period, in Figure 2c, the ionograms demonstrate that reflections from the auroral-type sporadic *Es* layer became highly scattered and spread in virtual altitude, and a slight stratification was observed in the 6–8 MHz frequency range. As the frequency increased, the reflection trace virtual height (distance) of the sporadic *Es* layer increased significantly, reaching up to 200 km. It is generally accepted that the auroral-type sporadic *Es* layer appears on ionograms as a scattered layer in altitude, with a characteristic increase in virtual height with frequency. This height variation is attributed to side reflections at greater distances, confirmed by DPS-4 data. The ionogram (see Figure 3c) shows that the directions of the scattered signals in the 7–8 MHz range correspond mainly to the northwest and northeast. Reflections from the southeast direction appear in the 7.5–8 MHz range. The sporadic *Es* layer continued to screen the upper layers.

Thus, data from the WD IZMIRAN observatory's instrument suite during the extremely strong Victory Day Geomagnetic Storm recorded large-scale auroral effects. Optical observations with the all-sky camera, radio diagnostics using the Parus-A ionosonde, and dual-frequency GNSS receivers data captured the following phenomena in the initial hours of the storm:

- PJ/SAID manifestations observed on ionograms and STEVE detected by the all-sky camera at 20:00 UT, lasting several minutes north of the observatory. At the same time, there was an increase in the ROTI by 1 TECU/min.
- Diffuse aurora with a moving omega structure observed from 20:43 to 20:47 UT, accompanied by a significant ROTI increase exceeding 4 TECU/min and enhanced scattering of the auroral *Es* layer on ionograms.
- Ray and corona auroral structures observed over the observatory from 22:26 to 23:02 UT, with the highest and most prolonged ROTI increase exceeding 4 TECU/min and *foEs* increase up to 10 MHz.

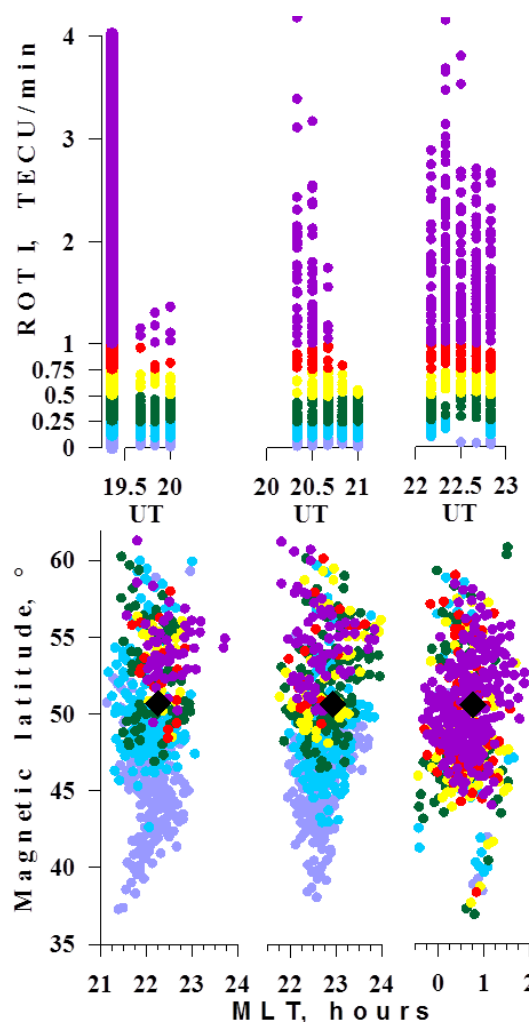


**Figure 4.** ROTI for 21 stations located between 50°–61°N and 15°–26°E (Kaliningrad/KLG1 54.36°; 20.12°) during three intervals on May 10, 2024: 19:40 – 20:20 UT (a), 20:20 – 21:00 UT (b), 22:10 – 22:50 UT (c). The color scale indicating changes in the ROTI is displayed in the left panel. The right panel shows the ROTI in MLT coordinates, with the location of the WD IZMIRAN Observatory in Kaliningrad highlighted by a black diamond.

### Satellite Data

This study uses data from the low-orbit satellites Swarm and DMSP to observe ionospheric plasma parameters during Victory Day 2024 Geomagnetic Storm.

Figure 5 illustrates time evolution of the electron density, electron temperature, horizontal ion drift velocity and vertical ion drift velocity measured in-situ by low-orbit satellites Swarm B and DMSP F-16 during Victory Day 2024 Storm. Instead of analyzing the large-scale characteristics of all measured ionospheric plasma parameters throughout the storm of May 10–12, we focused on the phenomena observed over the Kaliningrad region, where ground-based ionospheric plasma diagnostics facilities are located.

In particular, as will be shown below, the all-sky camera observed STEVE, which is closely associated with the Polarization Jet (PJ), also known as Subauroral Ion Drift (SAID), in the subauroral zone [Galperin et al., 1973; Spiro et al., 1979]. PJ/SAID is a narrow (1°–2° latitude) flow of intense (>1 km/s) westward ion drifts at altitudes of *F*-layer ionosphere. In addition to the features mentioned above, several other characteristics of PJ/SAID can serve as indirect indicators of its presence at a given time and location. These include the spatial alignment of a significant increase in horizontal ion drift velocity (>1 km/s), an electron density trough [Spiro et al., 1979], elevated electron temperature [Rodger et al., 1992], and an increase in vertical ion drift velocity [Khalipov et al., 2016]. PJ/SAID is

associated with subauroral optical phenomena such as STEVE [MacDonald *et al.*, 2018] and SAR-arcs [Cornwall *et al.*, 1971]. Moreover, the internal structure of PJ/SAID is not homogeneous [Sinevich *et al.*, 2022] and is often Stratified Subauroral Ion Drift (SSAID) with Polarization Jet Strata (PJS) [Sinevich *et al.*, 2023]. The sharp drop in electron density and plasma irregularities within PJ/SAID (or SSAID) can disrupt trans-ionospheric radio signals [Sinevich *et al.*, 2024a], potentially leading to degraded radio communications and navigational services [Kotova *et al.*, 2025].

The top panel of Figure 5 shows measurement results of Swarm B satellite in northern hemisphere at ~22 LT at 20 UT on May 10, 2024. The electron density trough ~1.25° wide lies between ~44.75° and ~46° geomagnetic latitudes and partially coincides with electron temperature rise which is ~0.75° wider in equatorial direction (44°–46°) and consists of two peaks at ~45.5° and at ~44.75° geomagnetic latitude, both approximately 0.5° wide. In accordance to abovementioned features, this electron density trough is a PJ/SAID. Note that ~45° geomagnetic latitude is not typical for PJ/SAID, the typical PJ/SAID location is within the 55°–70° [Spiro *et al.*, 1979] or 50°–65° [Karlsson *et al.*, 1998] geomagnetic latitude intervals. Location of the considered PJ/SAID this close to the equator is due to extremely high geomagnetic activity level during 2024 Victory Day geomagnetic storm (see Figure 1d, e). Since the PJ/SAID is usually located adjacent to the outer edge of the ionospheric projection of the plasmopause near equatorial boundary of auroral region, serious geomagnetic activity leads to significant shift of the plasmopause projection location closer to the equator. It is important to note that the electron density trough consists of two electron density dips at ~45.25° and at ~45.75° geomagnetic latitudes which are not as noticeable as electron temperature peaks and do not coincide spatially with them, nevertheless, have the approximately same latitudinal width (~0.5°). These electron density dips and electron temperature rise are probably large PJS and the PJ/SAID in question is SSAID [Sinevich *et al.*, 2023]. Electron density PJS and electron temperature PJS do not always spatially coincide [Sinevich *et al.*, 2024b]. Note that the satellite flew along the longitude of Kaliningrad region (~20°E) and 49°–51° geographic latitudes are close to the geographic latitude of West Department of IZMIRAN observatory.

Bottom panel of Figure 5 shows data from DMSP F-16 satellite in southern hemisphere at ~18 MLT at ~21 UT on May 10, 2024. Absence of electron density data is probably due to the fact that plasma density in this region during 2024 Victory Day geomagnetic storm is lower than sensitivity threshold of the instrument. Driftmeter data on board DMSP F-16 (horizontal and vertical ion drift velocity) explicitly indicates the presence of the PJ/SAID ~1.5° wide at –45.5°...–44° geomagnetic latitudes and its westward and upward ion drift velocity is up to ~1700 m/s and up to ~750 m/s respectively. Since the presence of PJ/SAID in southern hemisphere confirms the presence of PJ/SAID in northern hemisphere and vice versa [Anderson *et al.*, 1991] and PJ/SAID is typically stretched along the latitude from 18 to 02 LT at least [Karlsson *et al.*, 1998], the horizontal and vertical ion drift velocity peak at ~18 LT in southern hemisphere near –45° geomagnetic latitude additionally support that the PJ/SAID is present at ~22 LT in northern hemisphere in magnetically conjugated location near 45° geomagnetic latitude.

Thus, the satellite data are consistent with the ground-based measurements. According to the satellite data, it is clear that a PJ/SAID is developing in the initial phase of the extreme geomagnetic storm on May 10, 2024. It is also evident from the satellite data that during the storm activity, the auroral oval shifted to the geomagnetic equator and therefore the West Department of IZMIRAN observatory ended up in the auroral region. This made it possible to record omega structures, diffuse aurora and ray structure of polar lights in the Kaliningrad region which was accompanied by an increase in the ROTI.

## Discussion

This study examines the 2024 Victory Day geomagnetic storm, the most powerful geomagnetic event of the 21st century, which occurred on 10–12 May, affecting the ionosphere including subauroral and mid-latitude regions. The work uses ground-based facilities located in the Kaliningrad region, as well as satellite observations. Data from satellites,



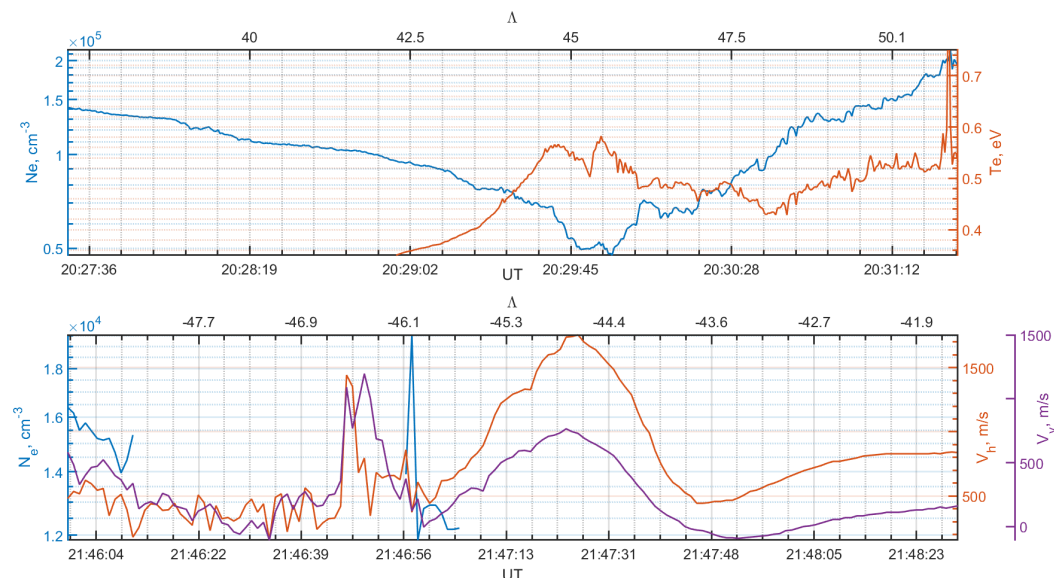


**Figure 5.** (Top panel) Evolution of the electron density (blue line,  $y$ -axis is on the left (logarithmic scale)) and electron temperature (red line,  $y$ -axis is on the right) measured by Swarm B at  $\sim 22$  LT at  $\sim 20$  UT on May 10, 2024. (Bottom panel) Evolution of horizontal (red line,  $y$ -axis is on the right) and vertical (purple line,  $y$ -axis is on the right) ion drift velocities, electron density (blue line,  $y$ -axis is on the left (logarithmic scale)) according to the DMSP F-16 data at  $\sim 21$  UT and  $\sim 18$  LT May 10, 2024. Here, geomagnetic latitude is the upper abscissa and UT is the lower abscissa.

ground-based ionosondes, GNSS receivers, and all-sky cameras recorded extensive changes in the near-Earth environment. Coronal mass ejections and the southern component of the interplanetary magnetic field played a key role in the occurrence of intense geomagnetic disturbances, as evidenced by sharp increases in solar wind velocity, plasma density, and extreme values of the  $AE$  and  $Dst$  geomagnetic indices. The resulting auroral expansions reached unexpected latitudes, which were recorded by ground-based facilities at the Ladushkin station near Kaliningrad. Unique optical phenomena such as STEVE, aurora and omega structure were observed over Kaliningrad during the peak activity, along with significant shifts in electron density and temperature recorded by various low-orbit satellites. This extreme storm also affected radio signals, which was confirmed by the ionosonde and GLONASS/GPS receivers. Main results are following:

- The most intense geomagnetic storm of the 21st century to date was primarily driven by coronal mass ejections and the southward component of the interplanetary magnetic field ( $B_z$ ), which initiated and intensified the event. The increase in solar wind speed, along with sharp rises in plasma density and temperature, indicated the presence of a shock wave before the storm's onset in the near-Earth plasma. This led to substantial geomagnetic and ionospheric effects, as evidenced by significant intense changes in the  $AE$  and  $Dst$  indices, expanding auroras to regions rarely affected and altering plasma distribution.
- PJ/SAID manifestations, detected using Swarm and DMSP satellite data, appeared on ionograms as a U-shaped structure, while STEVE, observed by the all-sky camera. During this time, the ROTI increased by 1 TECU/min.
- A diffuse aurora with a moving omega structure was seen, accompanied by a significant ROTI increase exceeding 4 TECU/min and enhanced scattering of the auroral  $E_s$  layer on ionograms.
- Ray and corona auroral structures were observed over the WD IZMIRAN observatory, coinciding with the highest and most prolonged ROTI rise, exceeding 4 TECU/min, and a  $foE_s$  increase of up to 10 MHz.

### Concluding Remarks

This study analyzes ionospheric irregularities during three geomagnetic storm intervals when STEVE, omega structures, rays, and corona auroral structures were observed over WD IZMIRAN, combining DMSP/Swarm satellite data with ground-based instruments. Our multi-source approach reveals how satellite measurements enhance ionosonde interpretation and track disturbance evolution, while all-sky cameras and satellites jointly connect optical phenomena with ionospheric irregularities. Key findings show storm-induced plasma inhomogeneities affecting radio propagation (ROTI variations), simultaneous STEVE events with U-shaped ionograms and ROTI spikes, and polarization jet/SAID formation during the May 2024 storm. Satellite data confirmed auroral oval expansion to Kaliningrad's latitude, enabling rare observations of omega structures, diffuse aurora and rays correlated with ROTI increases.

The study highlights the importance of analyzing space and ground-based observations to understand the effects of extreme geomagnetic storms and their impact on the ionosphere, especially for countries that are largely located in polar regions (e.g., Russia), and the shift of the auroral oval and the boundaries of subauroral and mid-latitude regions can lead to significant technological and technical slips and failures.

**Acknowledgements.** The DMSP data is available on the website <https://www.ngdc.noaa.gov/stp/satellite/satdataservices.html>. The Swarm data can be accessed through: <ftp://swarm-diss.eo.esa.int>. Geomagnetic activity index data is accessed from the World Geomagnetism Data Center in Kyoto <http://wdc.kugi.kyoto-u.ac.jp/Dstae/index.html>. Solar wind data is available on the website <https://services.swpc.noaa.gov>. The authors also thank J. H. King, N. Papatashvili at AdnetSystems, NASA GSFC and CDAWeb for providing the OMNI data ([http://cdaweb.gsfc.nasa.gov/istp\\_public/](http://cdaweb.gsfc.nasa.gov/istp_public/)). The work of AACH, AAS and DVCh on processing, interpretation and analysis of satellite data, geomagnetic indices was supported by the Russian Science Foundation (grant No. 25-12-00059).

### References

- Anderson P. C., Heelis R. A. and Hanson W. B. The ionospheric signatures of rapid subauroral ion drifts // *Journal of Geophysical Research: Space Physics*. — 1991. — Vol. 96, A4. — P. 5785–5792. — <https://doi.org/10.1029/90ja02651>.
- Bolduc L. GIC observations and studies in the Hydro-Québec power system // *Journal of Atmospheric and Solar-Terrestrial Physics*. — 2002. — Vol. 64, no. 16. — P. 1793–1802. — [https://doi.org/10.1016/S1364-6826\(02\)00128-1](https://doi.org/10.1016/S1364-6826(02)00128-1).
- Carmo C. S., Dai L., Wrasse C. M., et al. Ionospheric Response to the Extreme 2024 Mother's Day Geomagnetic Storm Over the Latin American Sector // *Space Weather*. — 2024. — Vol. 22, no. 12. — e2024SW004054. — <https://doi.org/10.1029/2024SW004054>.
- Carrington R. C. Description of a Singular Appearance seen in the Sun on September 1, 1859 // *Monthly Notices of the Royal Astronomical Society*. — 1859. — Vol. 20, no. 1. — P. 13–15. — <https://doi.org/10.1093/mnras/20.1.13>.
- Chernyshov A. A., Klimenko M. V., Nosikov I. A., et al. Effects in the upper atmosphere and ionosphere in the subauroral region during Victory Day 2024 Geomagnetic Storm (May 10-12, 2024) // *Advances in Space Research*. — 2025. — <https://doi.org/10.1016/j.asr.2025.02.015>.
- Cornwall J. M., Coroniti F. V. and Thorne R. M. Unified theory of SAR arc formation at the plasmopause // *Journal of Geophysical Research*. — 1971. — Vol. 76, no. 19. — P. 4428–4445. — <https://doi.org/10.1029/JA076i019p04428>.
- Galperin Y. I., Ponomarev V. N. and Zosimova A. G. Direct measurements of drift velocity of ions in the upper ionosphere during a magnetic storm. I. Methodical questions and some results of measurements during a magnetically quiet period of time // *Cosmic Research*. — 1973. — Vol. 11. — P. 273–283. — (In Russian).
- Gonzalez-Esparza J. A., Sanchez-Garcia E., Sergeeva M., et al. The Mother's Day Geomagnetic Storm on 10 May 2024: Aurora Observations and Low Latitude Space Weather Effects in Mexico // *Space Weather*. — 2024. — Vol. 22, no. 11. — e2024SW004111. — <https://doi.org/10.1029/2024sw004111>.
- Horvath I. and Lovell B. C. Traveling ionospheric disturbances and their relations to storm-enhanced density features and plasma density irregularities in the local evening and nighttime hours of the Halloween superstorms of 29-31 October 2003 // *Journal of Geophysical Research: Space Physics*. — 2010. — Vol. 115, A9. — A09327. — <https://doi.org/10.1029/2009JA015125>.

- Karlsson T., Marklund G. T., Blomberg L. G., et al. Subauroral electric fields observed by the Freja satellite: A statistical study // *Journal of Geophysical Research: Space Physics*. — 1998. — Vol. 103, A3. — P. 4327–4341. — <https://doi.org/10.1029/97JA00333>.
- Khalipov V. L., Stepanov A. E., Kotova G. A., et al. Vertical plasma drift velocities in the polarization jet observation by ground Doppler measurements and driftmeters on DMSP satellites // *Geomagnetism and Aeronomy*. — 2016. — Vol. 56, no. 5. — P. 535–544. — <https://doi.org/10.1134/s0016793216050066>.
- Kotova D. S., Sinevich A. A., Chernyshov A. A., et al. Strong turbulent flow in the subauroral region in the Antarctic can deteriorate satellite-based navigation signals // *Scientific Reports*. — 2025. — Vol. 15, no. 1. — P. 3458. — <https://doi.org/10.1038/s41598-025-86960-6>.
- MacDonald E. A., Donovan E., Nishimura Y., et al. New science in plain sight: Citizen scientists lead to the discovery of optical structure in the upper atmosphere // *Science Advances*. — 2018. — Vol. 4, no. 3. — <https://doi.org/10.1126/sciadv.aag0030>.
- Parnikov S. G., Ievenko I. B. and Koltovskoi I. I. Subauroral Luminosity STEVE over Yakutia during a Substorm: Analysis of the Event of March 1, 2017 // *Geomagnetism and Aeronomy*. — 2022. — Vol. 62, no. 4. — P. 434–443. — <https://doi.org/10.1134/S0016793222030136>.
- Pi X., Mannucci A. J., Lindqwister U. J., et al. Monitoring of global ionospheric irregularities using the Worldwide GPS Network // *Geophysical Research Letters*. — 1997. — Vol. 24, no. 18. — P. 2283–2286. — <https://doi.org/10.1029/97gl02273>.
- Rich F. J. and Denig W. F. The major magnetic storm of March 13-14, 1989 and associated ionosphere effects // *Canadian Journal of Physics*. — 1992. — Vol. 70, no. 7. — P. 510–525. — <https://doi.org/10.1139/p92-086>.
- Rodger A. S., Moffett R. J. and Quegan S. The role of ion drift in the formation of ionisation troughs in the mid- and high-latitude ionosphere-a review // *Journal of Atmospheric and Terrestrial Physics*. — 1992. — Vol. 54, no. 1. — P. 1–30. — [https://doi.org/10.1016/0021-9169\(92\)90082-V](https://doi.org/10.1016/0021-9169(92)90082-V).
- Sato N., Yukimatu A. S., Tanaka Y., et al. Morphologies of omega band auroras // *Earth, Planets and Space*. — 2017. — Vol. 69, no. 1. — <https://doi.org/10.1186/s40623-017-0688-1>.
- Sinevich A. A., Chernyshov A. A., Chugunin D. V., et al. Small-Scale Irregularities Within Polarization Jet/SAID During Geomagnetic Activity // *Geophysical Research Letters*. — 2022. — Vol. 49, no. 8. — e2021GL097107. — <https://doi.org/10.1029/2021GL097107>.
- Sinevich A. A., Chernyshov A. A., Chugunin D. V., et al. Stratified Subauroral Ion Drift (SSAID) // *Journal of Geophysical Research: Space Physics*. — 2023. — Vol. 128, no. 3. — <https://doi.org/10.1029/2022JA031109>.
- Sinevich A. A., Chernyshov A. A., Chugunin D. V., et al. Multi-Instrument Approach to Study Polarization Jet/SAID and STEVE // *Journal of Geophysical Research: Space Physics*. — 2024a. — Vol. 129, no. 11. — <https://doi.org/10.1029/2024JA033222>.
- Sinevich A. A., Chernyshov A. A., Chugunin D. V., et al. The Polarization Jet/SAID and Plasma Irregularities of Different Scales // *Bulletin of the Russian Academy of Sciences: Physics*. — 2024b. — Vol. 88, no. 3. — P. 375–380. — <https://doi.org/10.1134/S1062873823705548>.
- Spiro R. W., Heelis R. A. and Hanson W. B. Rapid subauroral ion drifts observed by Atmosphere Explorer C // *Geophysical Research Letters*. — 1979. — Vol. 6, no. 8. — P. 657–660. — <https://doi.org/10.1029/gl006i008p00657>.
- Stepanov A. E., Kobayakova S. E. and Khalipov V. L. Fast subauroral drifts of ionospheric plasma according to data from Yakut meridional chain of stations // *Solar-Terrestrial Physics*. — 2019. — Vol. 5, no. 4. — P. 60–65. — <https://doi.org/10.12737/stp-54201908>.
- Stone E. C., Frandsen A. M., Mewaldt R. A., et al. The Advanced Composition Explorer // *Space Science Reviews*. — 1998. — Vol. 86, no. 1–4. — P. 1–22. — <https://doi.org/10.1023/A:1005082526237>.
- Yasyukevich Yu. V., Vasiliev R. V., Rubtsov A. V., et al. Extreme Magnetic Storm of May 10-19, 2024: Coupling between Neutral and Charged Components of the Upper Atmosphere and the Effect on Radio Systems // *Doklady Earth Sciences*. — 2025. — Vol. 520, no. 2. — <https://doi.org/10.1134/S1028334X24604978>.